~~62 Copy 3 of 1~~ 489

[redacted]

NASA TM X-7

NASA TM X-7

[redacted]

TECHNICAL MEMORANDUM

X-7

DESIGN AND EXPERIMENTAL INVESTIGATION OF TWO ROTOR BLADE MODIFICATIONS FOR A HIGH-WEIGHT-FLOW, LOW-PRESSURE-RATIO TURBINE

By Robert R. Nunamaker, Donald A. Petrash
and Charles A. Wasserbauer

Lewis Research Center
Cleveland, Ohio

NATIONAL AERONAUTICS AND SPACE ADMINISTRATION

WASHINGTON September 1959

[redacted]

NATIONAL AERONAUTICS AND SPACE ADMINISTRATION

TECHNICAL MEMORANDUM X-7

DESIGN AND EXPERIMENTAL INVESTIGATION OF TWO ROTOR BLADE MODIFICATIONS FOR A HIGH-WEIGHT-FLOW, LOW-PRESSURE-RATIO TURBINE*

By Robert R. Nunamaker, Donald A. Petrash
and Charles A. Wasserbauer

SUMMARY

An over-all performance investigation was conducted on a high-weight-flow, low-pressure-ratio, single-stage turbine for use in a turbojet engine designed for a cruise Mach number of 4.0. As a continuation of this program, the effect on turbine over-all performance of two rotor blade modifications was investigated. The purpose of these modifications was to improve the mechanical characteristics of rotor blades that were thin in cross section and had a large blade height with a slight taper. Two rotor blade modifications were investigated. The first incorporated pinning of adjacent rotor blades in the tip region to link and support the rotor assembly mechanically. This turbine had a rating efficiency of 0.79, which is 0.04 below the design value at the equivalent design operating point. The equivalent design weight flow was not obtained by this rotor configuration. The second rotor blade configuration consisted of a rotor blade that had been redesigned with a greater consideration for its mechanical characteristics. This modification had essentially no detrimental effect on the over-all turbine performance at the equivalent design operating point.

INTRODUCTION

The requirements of a turbine for use in a low-pressure-ratio, high-weight-flow turbojet engine designed for a cruise Mach number of 4.0 have been investigated at the Lewis Research Center. The aerodynamic design method together with the results of a cold-air experimental performance investigation for an initial turbine configuration is presented in reference 1. In the design of this turbine configuration, the diffusion of the suction-surface velocity was kept to a minimum. This turbine, which

*Title, Unclassified.

will be referred to herein as configuration I, passed equivalent design weight flow at equivalent design work output and speed. The rating efficiency at this point was essentially the estimated design value of 0.83.

Rotor blade configuration I had a relatively thin cross section and a large blade height with a slight taper from hub section to tip section. In the first design, the emphasis was on desirable aerodynamic characteristics, whereas the structural properties of the blade were largely ignored. This established an upper limit of aerodynamic performance that could be expected from this class of turbine. The combined stresses that would be obtained in this rotor blade under actual operating conditions in a full-scale turbojet engine were considered dangerously high. Rotor blade fatigue failure due to vibration could occur in the regions of the hub section and the long, thin trailing edge near the tip section. Consideration of the possible fatigue failure caused by vibration at these critical areas necessitated an investigation of methods to improve the mechanical characteristics of the rotor blade. In the present report, an investigation of these methods was made to determine what sacrifice in performance would be associated with each method.

Two methods of improving the mechanical characteristics were investigated to determine their individual effect on the turbine over-all performance. The first method consisted of the introduction of 0.120-inch-diameter stainless-steel pins into the blade flow passage and the linkage of these pins to adjacent rotor blades, thus supporting each rotor blade to satisfy structural stability. Hereafter, this rotor blade will be called rotor blade configuration II. In the second method the rotor blade was redesigned to include a higher blade camber at the outer radii, a decreased cross-sectional area at the tip section, and an increase of the hub-section area, thereby lowering the combined stresses associated with the rotor blade during operation. This rotor blade will be referred to as rotor blade configuration III for this investigation.

The purpose of this experimental investigation is to determine the effect on the turbine aerodynamic over-all performance characteristics caused by the modifications to the rotor blades to improve the mechanical properties. All rotor blades used in the cold-air experimental performance investigation were fabricated from aluminum stock. The two rotor blade configuration designs are described, and their individual effects on the turbine over-all performance are presented.

SYMBOLS

D_p pressure-surface diffusion parameter,

$$\frac{\text{(blade-inlet relative velocity) - (min. blade surface relative velocity)}}{\text{(blade-inlet relative velocity)}}$$

D_s suction-surface diffusion parameter,

$$\frac{\text{(max. blade surface relative velocity) - (blade-outlet relative velocity)}}{\text{(max. blade surface relative velocity)}}$$

D_{tot} sum of suction- and pressure-surface diffusion parameters, $D_p + D_s$

E specific work output (based on measured torque), Btu/lb

g gravitational constant, 32.17 ft/sec^2

N rotational speed, rpm

p absolute pressure, lb/sq ft

Q torque, ft-lb

r radius, ft

T absolute temperature, ^oR

U blade velocity, ft/sec

V_{cr} critical velocity at NASA standard sea-level temperature of 518.7° R

W relative gas velocity, ft/sec

w weight flow, lb/sec

γ ratio of specific heats

δ ratio of inlet total pressure to NASA standard sea-level pressure of 2116 lb/sq ft

ϵ function of $\gamma, \frac{\gamma_{sl}}{\gamma}\left[\frac{\left(\frac{\gamma+1}{2}\right)^{\frac{\gamma}{\gamma-1}}}{\left(\frac{\gamma_{sl}+1}{2}\right)^{\frac{\gamma_{sl}}{\gamma_{sl}-1}}}\right]$

η aerodynamic efficiency, ratio of actual turbine work (based on torque measurements) to ideal turbine work (based on exit total pressure p'_3)

η_x rating efficiency, ratio of actual turbine work (based on torque measurements) to ideal turbine work (based on exit total pressure $p'_{3,x}$)

θ_{cr} squared ratio of critical velocity to critical velocity at NASA standard sea-level temperature of 518.7° R

σ blade solidity based on axial chord

Subscripts:

p pressure surface

s suction surface

sl NASA standard sea-level conditions

t tip

tot total

x axial

0,1,2,3 measuring stations, see fig. 2

Superscript:

' total or stagnation state

APPARATUS AND PROCEDURE

Test Installation and Instrumentation

The experimental test installation of the turbine is shown in figure 1. This test facility is the same as the one used to experimentally investigate the turbine with rotor blade configuration I, which is described in detail in reference 1.

The instrumentation used for the over-all performance evaluation of the turbine is identical to the instrumentation used in reference 1. A schematic diagram of the experimental setup and the measuring stations is shown in figure 2.

Experimental Procedure

The turbine was operated with a measured inlet total pressure of approximately 40 inches of mercury absolute and a nominal inlet total temperature T_0' of 540° R. Turbine rotative speeds of 60 to 120 percent equivalent design speed in 10-percent increments were used over a range of rating pressure ratio $p_1'/p_{3,x}'$ from 1.3 to 1.75.

The operating conditions, facility instrumentation, and experimental data reduction methods used to investigate these turbines experimentally are identical to those described in reference 1.

TURBINE DESIGN

It was desired to design a turbine having high weight flow per unit frontal area with relatively low specific work output while, at the same time, maintaining good aerodynamic efficiency and good structural characteristics.

The cold-air-model single-stage turbine used in this investigation is 16 inches in diameter and has a constant hub-tip radius ratio of 0.53. The over-all design requirements for the turbine are as follows:

Equivalent specific work output, E/θ_{cr}, Btu/lb	12.22
Equivalent weight flow, $\frac{w\sqrt{\theta_{cr}}}{\delta}\epsilon$, lb/sec	28.09
Equivalent blade tip speed, $U_t/\sqrt{\theta_{cr}}$, ft/sec	520

The velocity diagrams used in the design of the turbines for this investigation are the same as those presented in figure 1 of reference 1. The stator blade used with configuration I (ref. 1) was also used with configurations II and III in the present turbine investigation. The rotor blade design of configuration I was considered undesirable from the standpoint of mechanical stresses. In the region of the tip, the blade had a long thin straight trailing edge which would be subject to vibrational fatigue failure. The combined centrifugal and bending stresses at the hub section of this blade, which has relatively little taper, were also quite high. Two methods are considered in the present study to alleviate these mechanical-stress problems. The first method is a modification in which pins were used to link adjacent blades of rotor blade configuration I together in order to dampen any vibration of the blades. The second method for improving the mechanical characteristics of the blades is to redesign them by adding curvature near the trailing edge in the region of the tip, which would thus stiffen this section. The thickness of the blade profile was increased at the hub section and decreased at the tip section, which gave the blade a greater hub- to tip-section-area ratio and improved the centrifugal stress characteristics.

Description of Rotor Blade for Configuration II

The rotor blade configuration II assembly is shown in figures 3 and 4. The pins that mechanically linked adjacent blades were 0.120-inch stainless-steel tubing cut to lengths of approximately 1 inch. These pins were sealed to prevent any crossflow through the pins.

As shown in the figures, the pins were located near the throat of the rotor blade at three-fourths the blade height in order to dampen blade vibration by supporting the long thin trailing edge in the region of the tip section. For maximum damping the pins should have been located as near the tip section as possible; however, to satisfy stress considerations the three-fourths blade height location was chosen. The pins, when in position, extended through the blade. This allowed them to be held in position by snap rings that were fitted on the pin body and pushed snugly against the blade surface. Although constant-diameter pins of this type would be unsuitable for use in a full-scale high-temperature turbine, the approximate aerodynamic blockage that would be caused by proposed pins for an actual turbine was scaled so that the effect on the aerodynamic performance could be determined in the cold-air-model turbine investigation.

Since rotor blade configuration II is a modification of configuration I, the values of suction- and pressure-surface diffusion remain unchanged for the basic rotor blade. No attempt was made to estimate the diffusion parameters for the complex surface flow patterns set up from

the addition of the pins. The coordinates of the blade hub, mean, and tip sections for this rotor blade are shown in table II(b) of reference 1.

Rotor Blade Design for Configuration III

The design procedure for rotor blade configuration III differed from the design procedure used for rotor blade configuration I, in that greater consideration was provided for the mechanical stresses and vibrational characteristics of the rotor blade. Rotor blade configuration III is shown in figure 4.

Curvature of the blade mean camber line in the region of the trailing edge was introduced, thereby stiffening the rotor blade. The turning downstream of the throat was approximately 6°, 3°, and 0° at the tip, mean, and hub sections, respectively. The change in the blade sections is illustrated in figure 5 where the hub, mean, and tip sections of rotor blade configuration III are superimposed over the similar sections of rotor blade configuration I.

The tip-section area of rotor blade configuration III was reduced, and the hub-section area was increased to reduce the centrifugal stresses at the hub of the blade. The hub- to tip-section-area ratio for rotor blade configuration I was approximately 1.8 to 1. The similar ratio for rotor blade configuration III was approximately 3.0 to 1.

The results obtained in references 2 and 3 indicate that low suction-surface diffusion is desirable for minimum over-all losses through a turbine-rotor blade row. Therefore, because it was desired to maintain zero suction-surface diffusion, when the rotor blade profiles were changed, the pressure-surface diffusion was increased as shown in table I. This table also compares the values for the hub, mean, and tip sections of rotor blade configuration III with those for rotor blade configuration I. As shown in table I, the suction-surface diffusion values remained essentially unchanged during the redesign process.

The velocity distribution on the midchannel line and the blade surfaces at the hub, mean, and tip sections for blade configuration III are presented in figure 6. The coordinates of the blade hub, mean, and tip sections for this rotor blade are shown in table II. The final blade shape was obtained by stacking the hub-, mean-, and tip-section profiles so that the centers of gravity at the three sections were on a radial line in order to reduce the combined stresses.

RESULTS AND DISCUSSION

The over-all turbine performance obtained with rotor blade configurations II and III is individually presented. These results are then compared with those obtained with configuration I, the rotor designed for optimum aerodynamic performance.

Performance of Rotor Blade Configuration II

The over-all performance of the turbine for this configuration is presented in figure 7(a) where equivalent work output is plotted against the weight-flow parameter $\frac{wN}{60\delta}\epsilon$ for constant values of equivalent speed and rating pressure ratio $p_1'/p_{3,x}'$. Contours of constant rating efficiency η_x based on the rating pressure ratio $p_1'/p_{3,x}'$ are shown.

At equivalent design work output and speed, an efficiency of 0.79 was obtained. This corresponded to a rating pressure ratio of 1.6. A maximum value of efficiency of 0.83 was obtained at low pressure ratios near design speed.

In order to present a more complete evaluation of the turbine performance, a performance map with the efficiencies of the turbine based on the over-all pressure ratio p_1'/p_3' is presented in figure 7(b).

At equivalent design work output and speed, an aerodynamic efficiency of 0.81 is obtained at a pressure ratio p_1'/p_3' of 1.57. This efficiency is 0.02 higher than the rating efficiency based on the rating pressure ratio $p_1'/p_{3,x}'$. This difference in efficiency indicates the loss in energy caused by the tangential velocity component at the turbine exit.

The variation of equivalent weight flow with rating pressure ratio for the equivalent speeds investigated is shown in figure 8(a). The value for equivalent design weight flow is indicated. At equivalent design speed and a rating pressure ratio of 1.59 corresponding to equivalent design work, the measured turbine weight flow was about 1 percent below the design value. Choking weight flow was obtained above a rating total-pressure ratio of 1.65 for the 60 and 70 percent design rotor speeds investigated only. At the rating total-pressure ratio of 1.73, the highest pressure ratio investigated, choking weight flow was very nearly obtained for the remaining speeds. In figure 8(a) the value of choking weight flow remains constant for the 60 and 70 percent design rotor speeds, which indicates that the stator choked for these speeds prior to the rotor and controlled the weight flow passed by the turbine. At turbine rotor speeds greater than the low rotor speeds, the value of

choking weight flow decreases, which indicates that the rotor blade row chokes initially and limits the turbine weight flow.

The variation of equivalent torque with rating pressure ratio for the equivalent speeds investigated is shown in figure 8(a). Pressure ratios across the turbine great enough to achieve limiting loading were not obtainable. Limiting loading for any given speed is defined as the point at which a further increase in pressure ratio does not produce an increase in torque.

Performance of Rotor Blade Configuration III

The performance of this turbine, presented in figure 9, was limited to equivalent design speed for a variation of rating total-pressure ratios due to a rotor blade fatigue failure during the experimental investigation. The fact that this rotor blade did fail during the experimental investigation was attributed to the characteristics of the test facility. The rotor blades were fabricated from aluminum stock which did not give the blades the proper structural stability when the unfavorable test condition was encountered. However, because it is the effect on aerodynamic performance and not the stability of the scaled model in a cold-air test that is important for this investigation, the limited performance data are presented herein.

Only five experimental points were obtained. Figure 9 shows the variation of rating efficiency η_x with equivalent turbine work output for equivalent design speed only. In addition, similar curves for rotor blade configurations I and II are shown for comparison and will be discussed later.

At equivalent design work output and speed, a rating efficiency of 0.825 was obtained. This corresponded to a rating pressure ratio of slightly greater than 1.55. A maximum value of 0.847 was obtained at a low pressure ratio of 1.34 at design speed.

At equivalent design work output and speed, an aerodynamic efficiency of 0.828 was obtained at a total-pressure ratio p_1'/p_3' of 1.55. This efficiency is 0.003 higher than the efficiency based on the rating pressure ratio $p_1'/p_{3,x}'$, which indicates that the exit tangential velocity component is negligible.

The variation of equivalent weight flow with rating pressure ratio for equivalent design speed is shown in figure 9. At equivalent design speed and a rating pressure ratio of 1.55 corresponding to equivalent design and work output, the measured turbine weight flow was slightly higher than the design value. No presentation can be given concerning choking weight flow for this rotor blade because of the limited amount of data that was obtained.

The variation of equivalent torque with rating pressure ratio for design speed is shown in figure 9. A pressure ratio across the turbine great enough to achieve limiting loading was not obtainable.

Effect of Rotor Blade Modifications on Turbine Performance

The rating efficiency at design blade speed for the three configurations over a range of work output is compared in figure 9.

The rating efficiency at equivalent design work output and speed for rotor blade configuration II of 0.79 represents a decrease of 0.04 from rotor blade configuration I (fig. 9). The turbine weight flow for rotor blade configuration II was approximately 1 percent below the design value which was obtained by the aerodynamically designed rotor blade of configuration I. The pins used to support the rotor blades mechanically produced an air blockage within the blade flow passage. This flow blockage produced losses that account for the reduced efficiency and weight flow.

The rating efficiency for rotor blade configuration III shows essentially no change in efficiency from rotor blade configuration I (fig. 9). The turbine weight flow of this configuration did reach the design equivalent value as did the turbine weight flow for rotor blade configuration I. The fact that this rotor blade configuration failed during the experimental investigation was attributed to characteristics of the test facility and stress concentrations near the base of the aluminum blades.

SUMMARY OF RESULTS

The following results were obtained from an experimental investigation of two rotor blade configurations for a high-weight-flow, low-pressure-ratio, single-stage turbine. The turbine was operated over a range of equivalent speed and pressure ratio at inlet conditions of 40 inches of mercury absolute and 80° F.

The use of pins between adjacent rotor blades to dampen stresses due to vibration caused a considerable change in the turbine over-all performance from that previously obtained for an aerodynamically designed rotor blade. At the design operating conditions the rating efficiency was decreased 0.04, and the turbine weight flow was decreased approximately 1 percent.

The performance of the redesigned rotor blade in which the blades were tapered to reduce centrifugal stresses at the hub was essentially

the same as the aerodynamically designed rotor blade. At the design operating conditions the rating efficiency was the design value, and the design weight flow was obtained.

Lewis Research Center
National Aeronautics and Space Administration
Cleveland, Ohio, January 16, 1959

REFERENCES

1. Petrash, Donald A., Nunamaker, Robert R., and Wasserbauer, Charles A.: Design and Experimental Investigation of a High-Weight-Flow Low-Pressure-Ratio Turbine. NASA TM X-6, 1959.

2. Nusbaum, William J., Wasserbauer, Charles A., and Hauser, Cavour H.: Experimental Investigation of a High Subsonic Mach Number Turbine Having a 40-Blade Rotor with Zero Suction-Surface Diffusion. NACA RM E57J22, 1958.

3. Nusbaum, William J., and Wasserbauer, Charles A.: Experimental Investigation of a High Subsonic Mach Number Turbine Having a 32-Blade Rotor with Low Suction-Surface Diffusion. NASA MEMO 10-2-58E, 1958.

TABLE I. - SURFACE DIFFUSION AND SOLIDITY PARAMETERS

FOR ROTOR BLADES

Rotor blade	Section	Blade surface diffusion parameter			Solidity, σ
		Suction surface, D_s	Pressure surface, D_p	D_{tot}	
Configuration I (ref. 1)	Hub	0	0.50	0.50	2.71
	Mean	0.10	0.43	0.53	1.59
	Tip	0	0.22	0.22	0.99
Configuration III	Hub	0	0.84	0.84	2.71
	Mean	0.10	0.57	0.67	1.59
	Tip	0	0.50	0.50	0.99

TABLE II. - ROTOR BLADE CONFIGURATION III SECTION COORDINATES

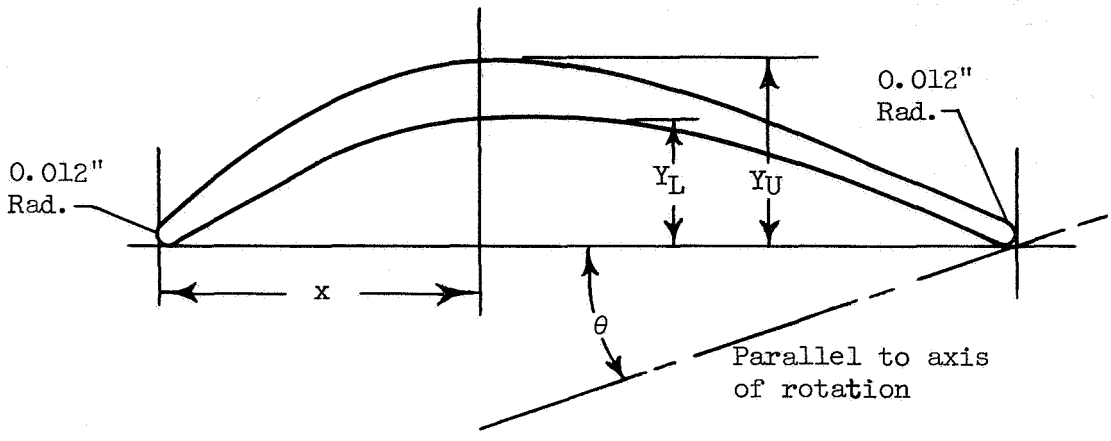

x, in.	Hub		Mean		Tip	
	$\theta = -5^\circ 0'$ $r/r_t = 0.533$		$\theta = 13^\circ 46'$ $r/r_t = 0.766$		$\theta = 34^\circ 10'$ $r/r_t = 1.000$	
	Y_L, in.	Y_U, in.	Y_L, in.	Y_U, in.	Y_L, in.	Y_U, in.
0.000	0.012	0.012	0.012	0.012	0.012	0.012
.100	.060	.123	.051	.102	.025	.065
.200	.123	.213	.099	.173	.045	.092
.300	.175	.236	.133	.216	.056	.104
.400	.214	.340	.155	.235	.061	.107
.500	.239	.373	.162	.235	.059	.101
.600	.252	.385	.158	.219	.054	.090
.700	.252	.376	.141	.189	.044	.077
.800	.241	.347	.115	.152	.032	.062
.900	.217	.300	.080	.111	.017	.045
1.000	.179	.242	.040	.068	----	----
1.034	----	----	----	----	.012	.012
1.100	.128	.171	----	----	----	----
1.106	----	----	.012	.012	----	----
1.200	.066	.098	----	----	----	----
1.306	.012	.012	----	----	----	----

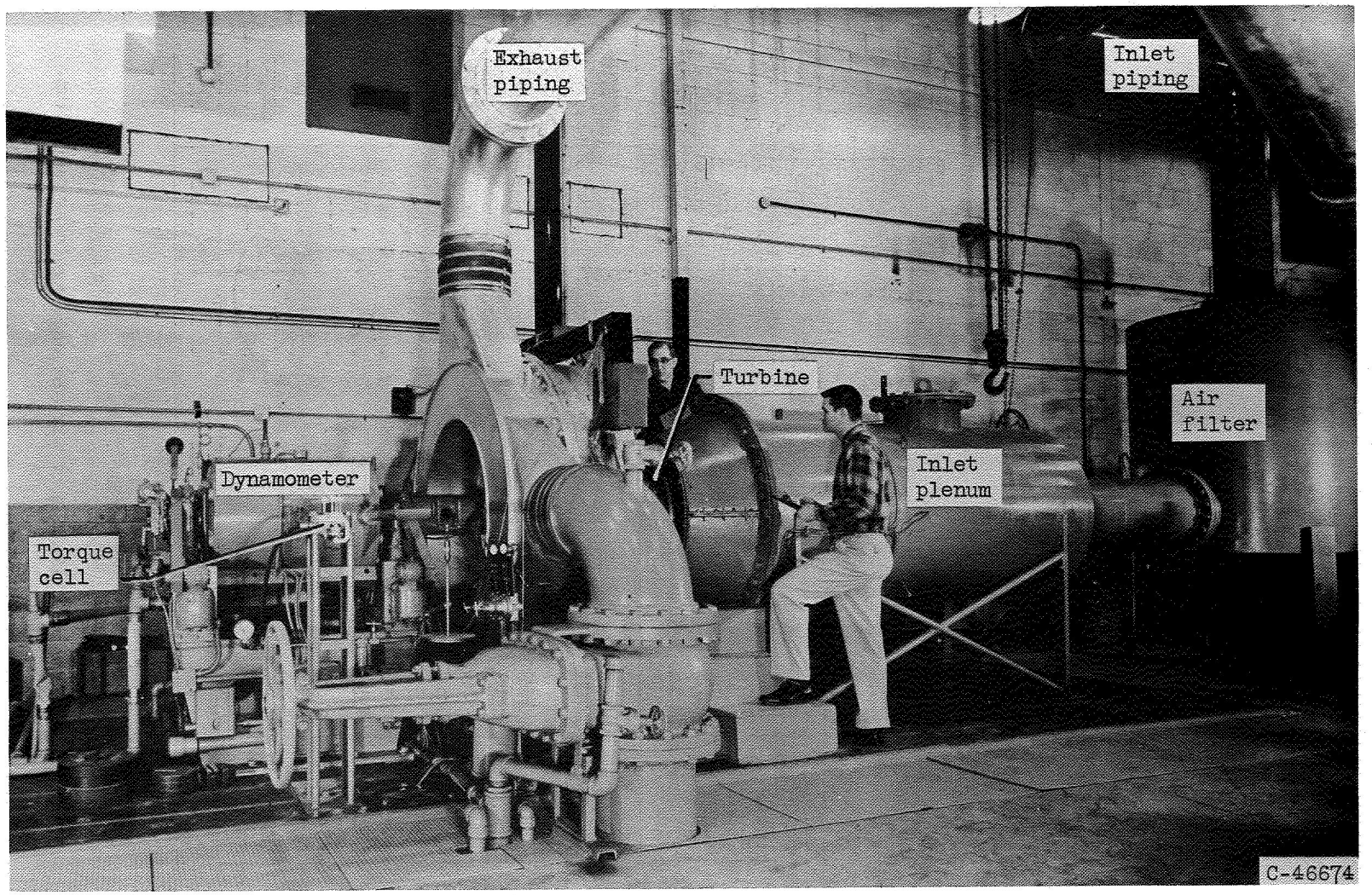

Figure 1. - Installation of turbine in cold-air turbine-component test facility.

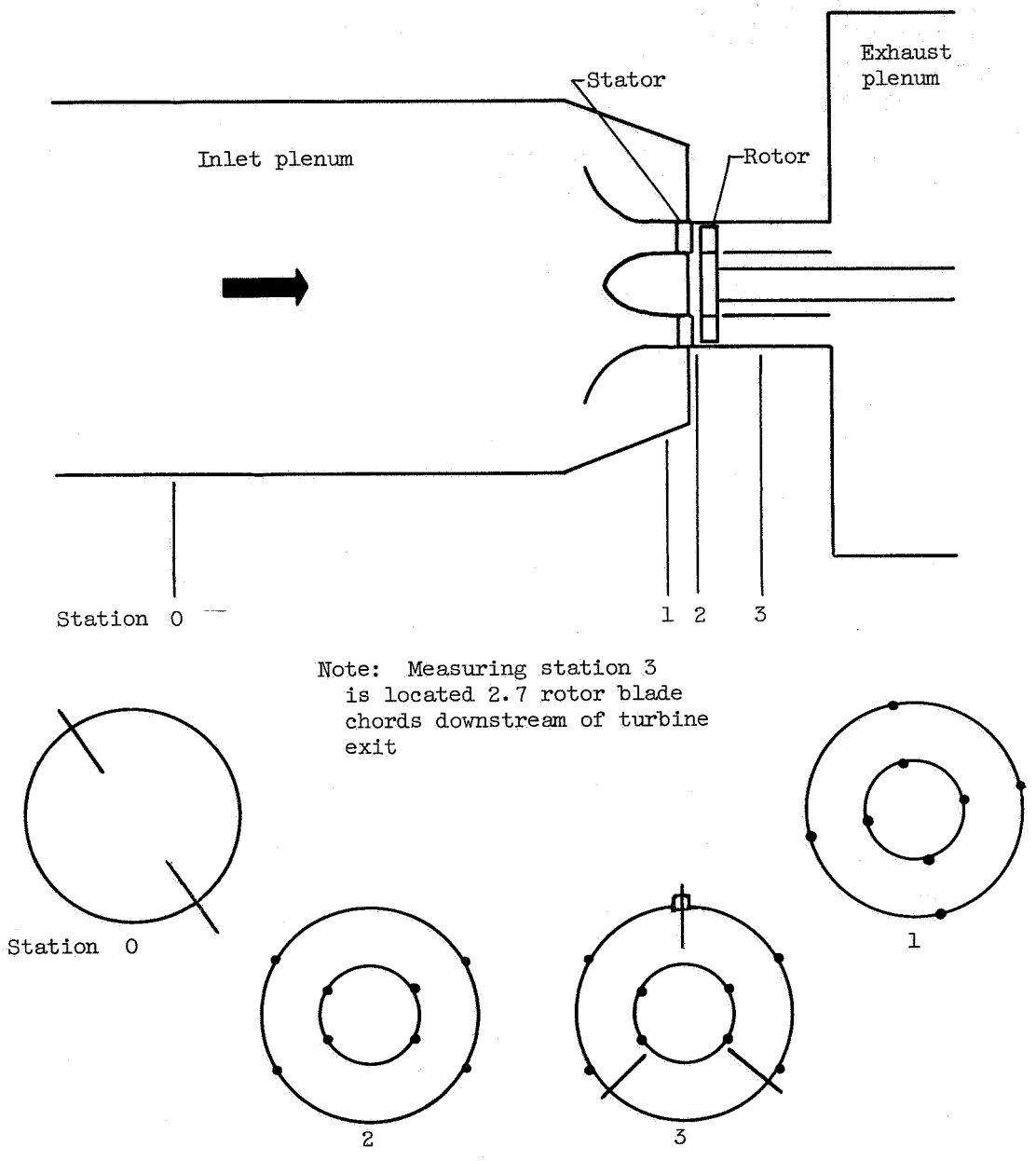

Figure 2. - Schematic diagram of turbine showing instrumentation.

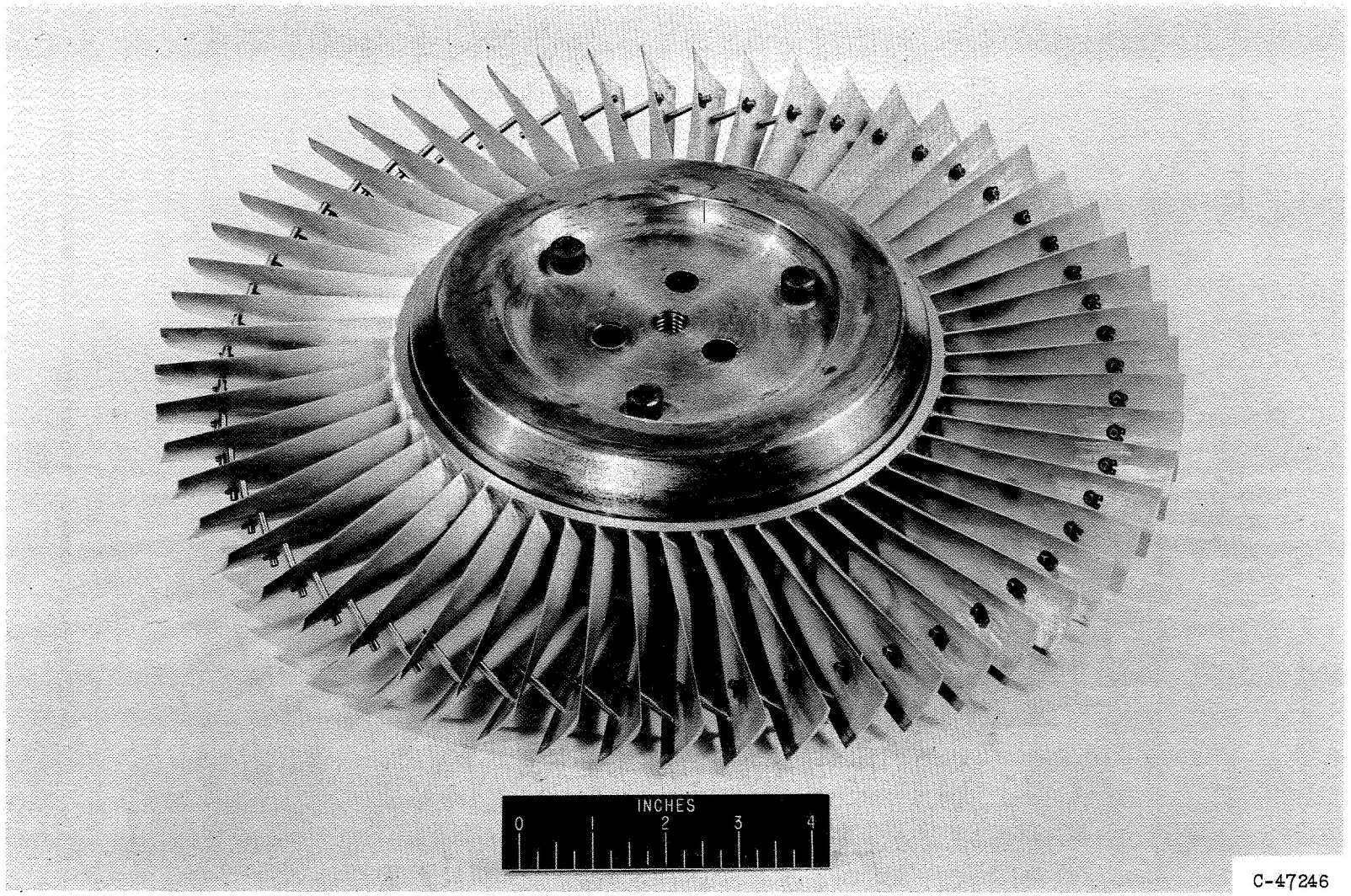

(a) Over-all view.

Figure 3. - Rotor blade configuration II.

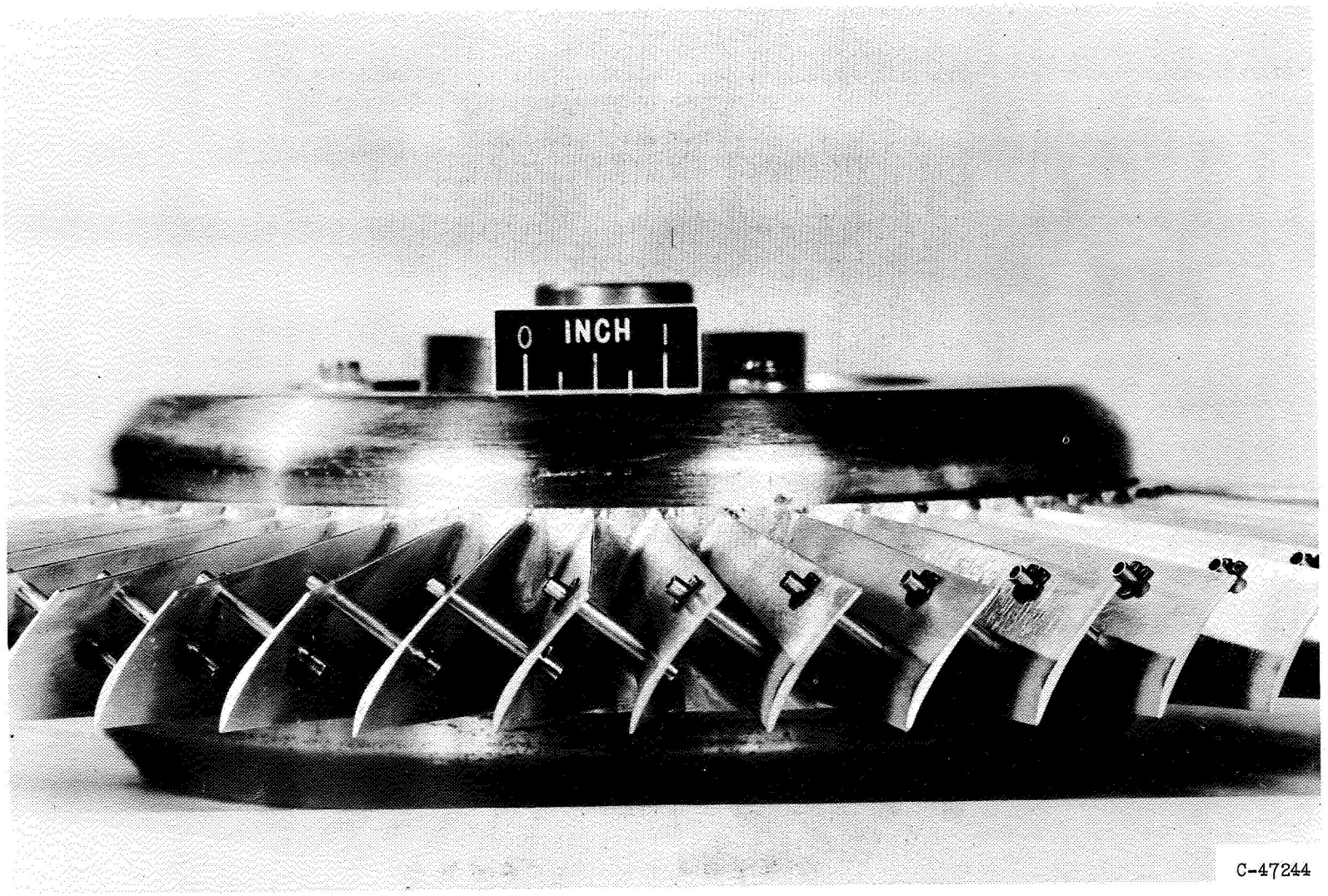

(b) Closeup view showing pin.

Figure 3. - Concluded. Rotor blade configuration II.

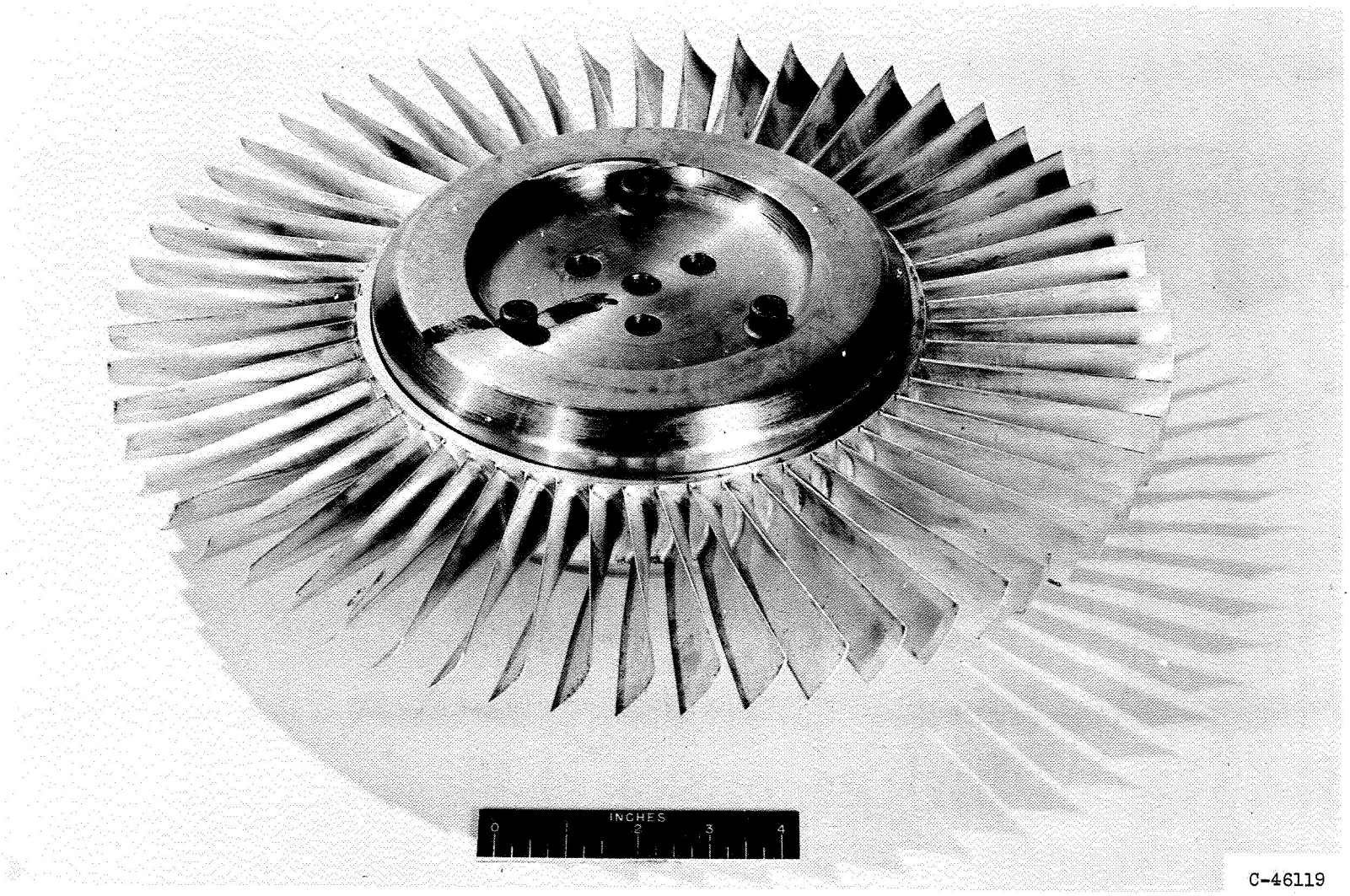

Figure 4. - Rotor blade configuration III.

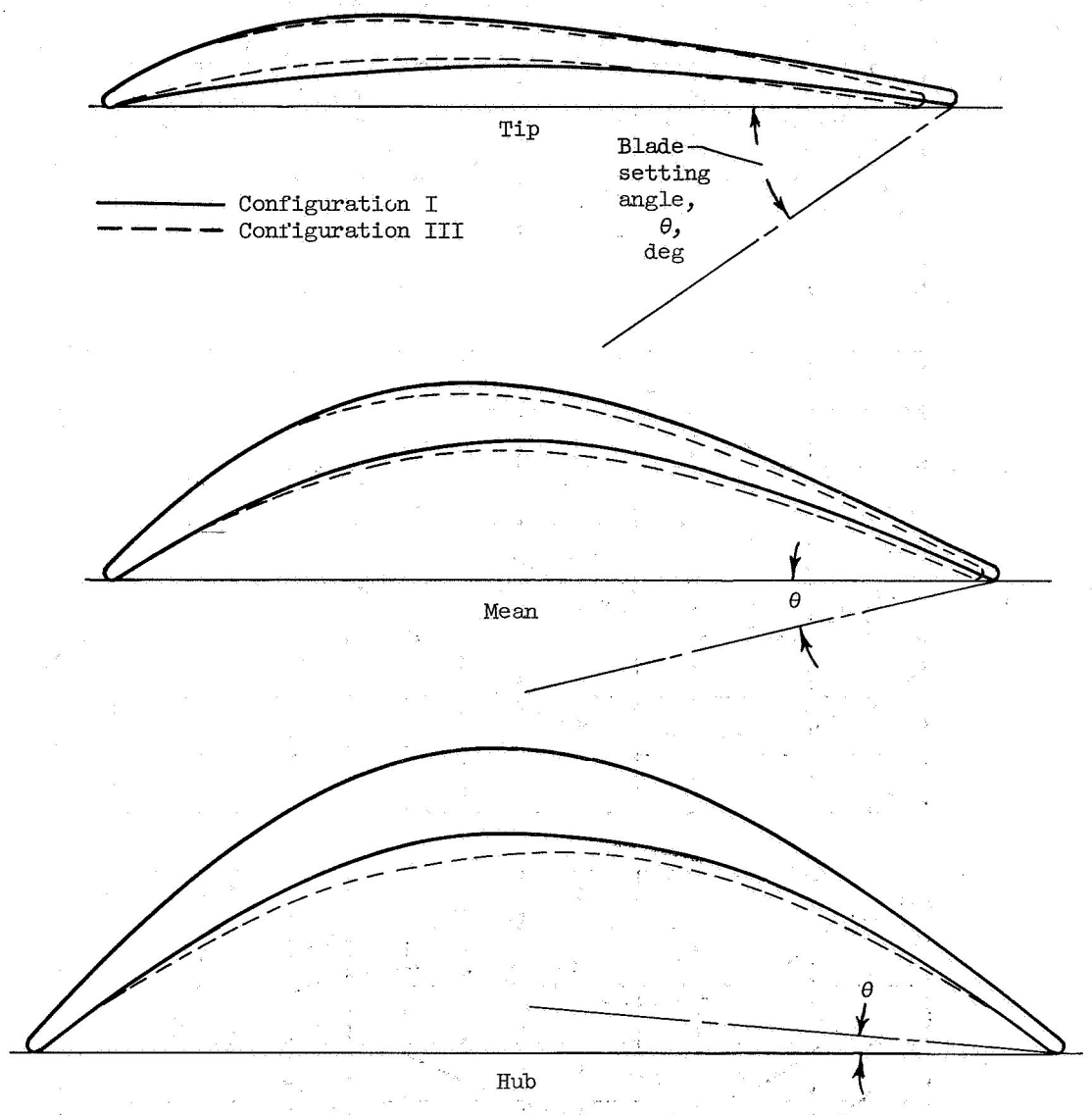

Figure 5. - Profile comparison between rotor blade configurations I and III.

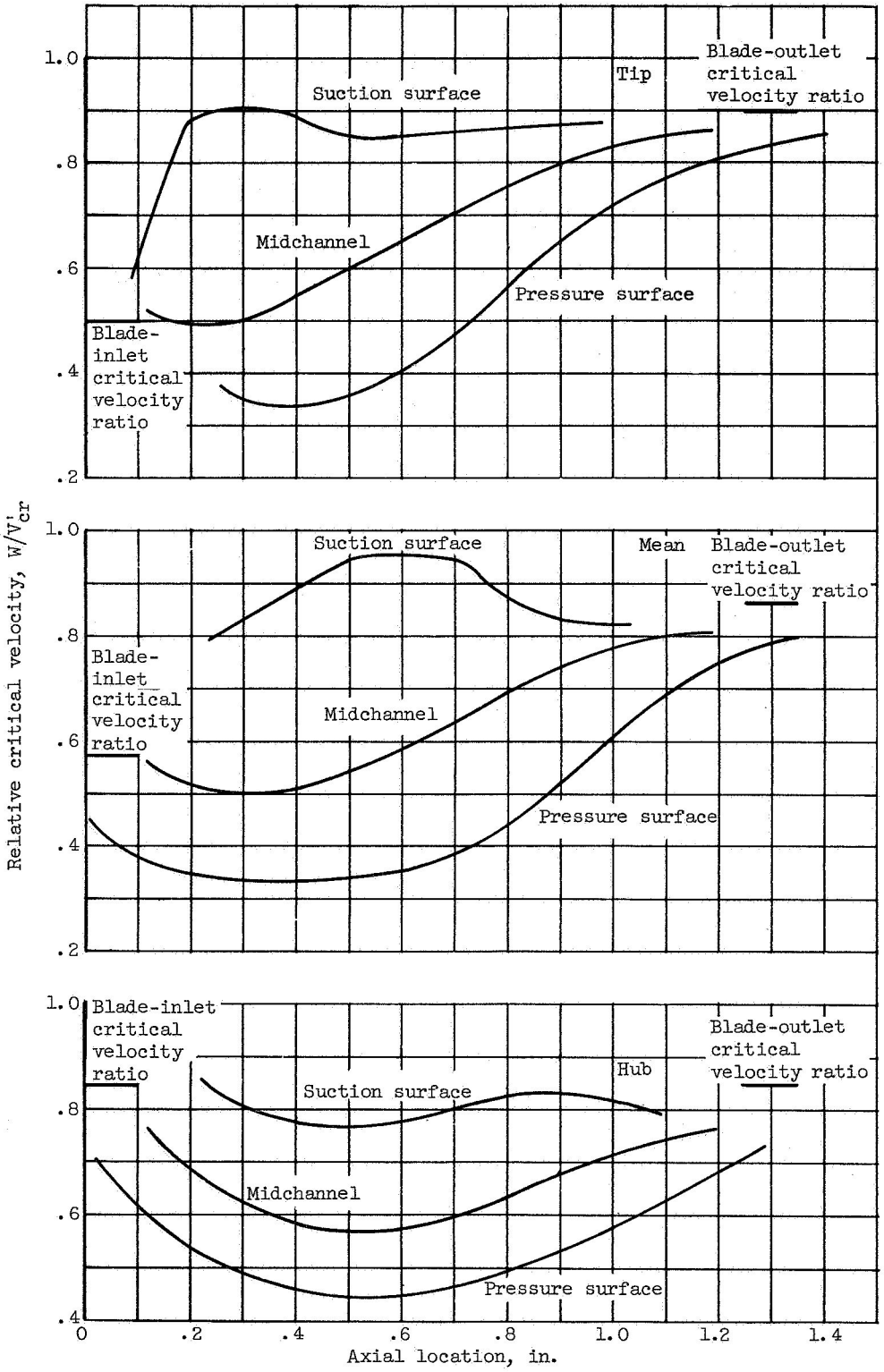

Figure 6. - Design rotor blade midchannel and surface velocity distribution at hub, mean, and tip sections as a function of axial location. Rotor blade configuration III.

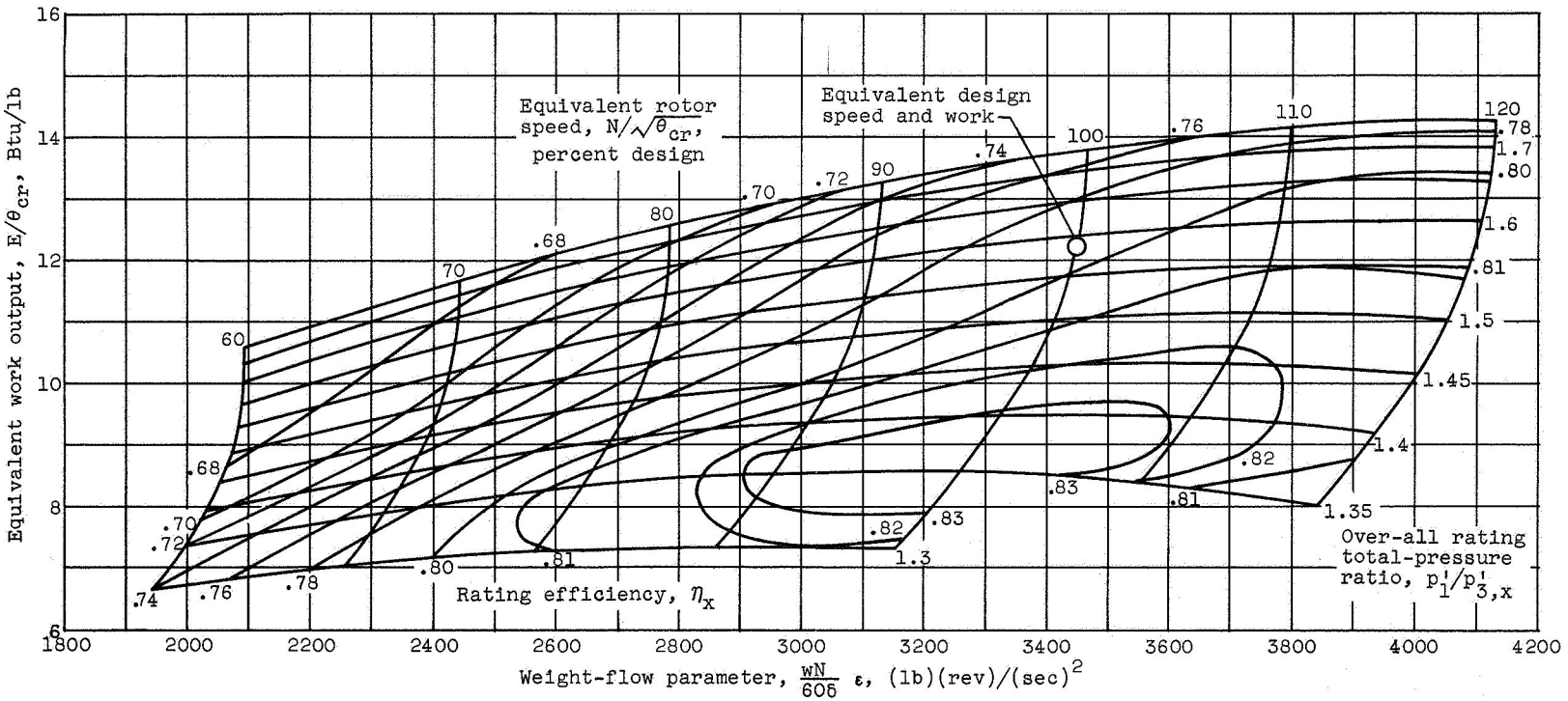

(a) Rating efficiency basis.

Figure 7. - Over-all performance of turbine with rotor blade configuration II.

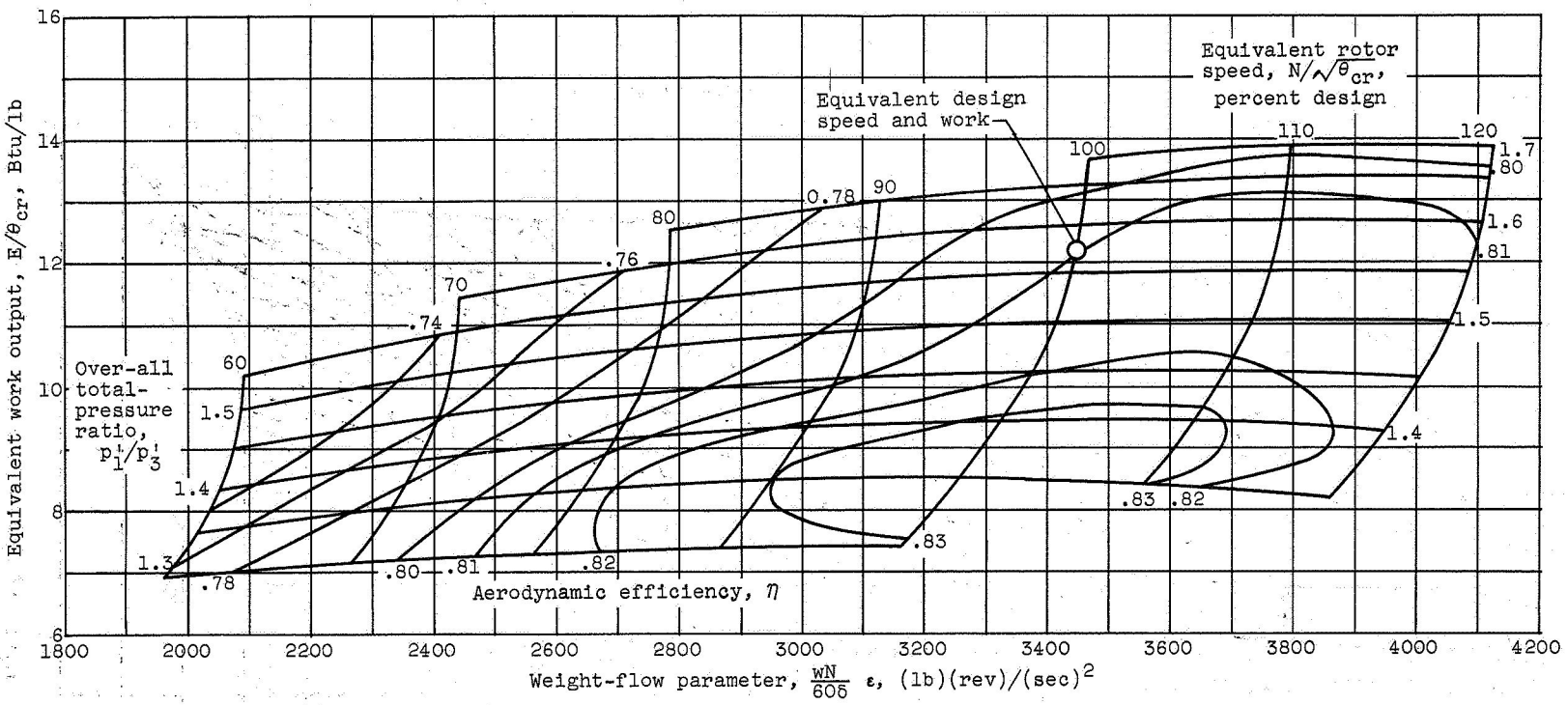

(b) Aerodynamic efficiency basis.

Figure 7. - Concluded. Over-all performance of turbine with rotor blade configuration II.

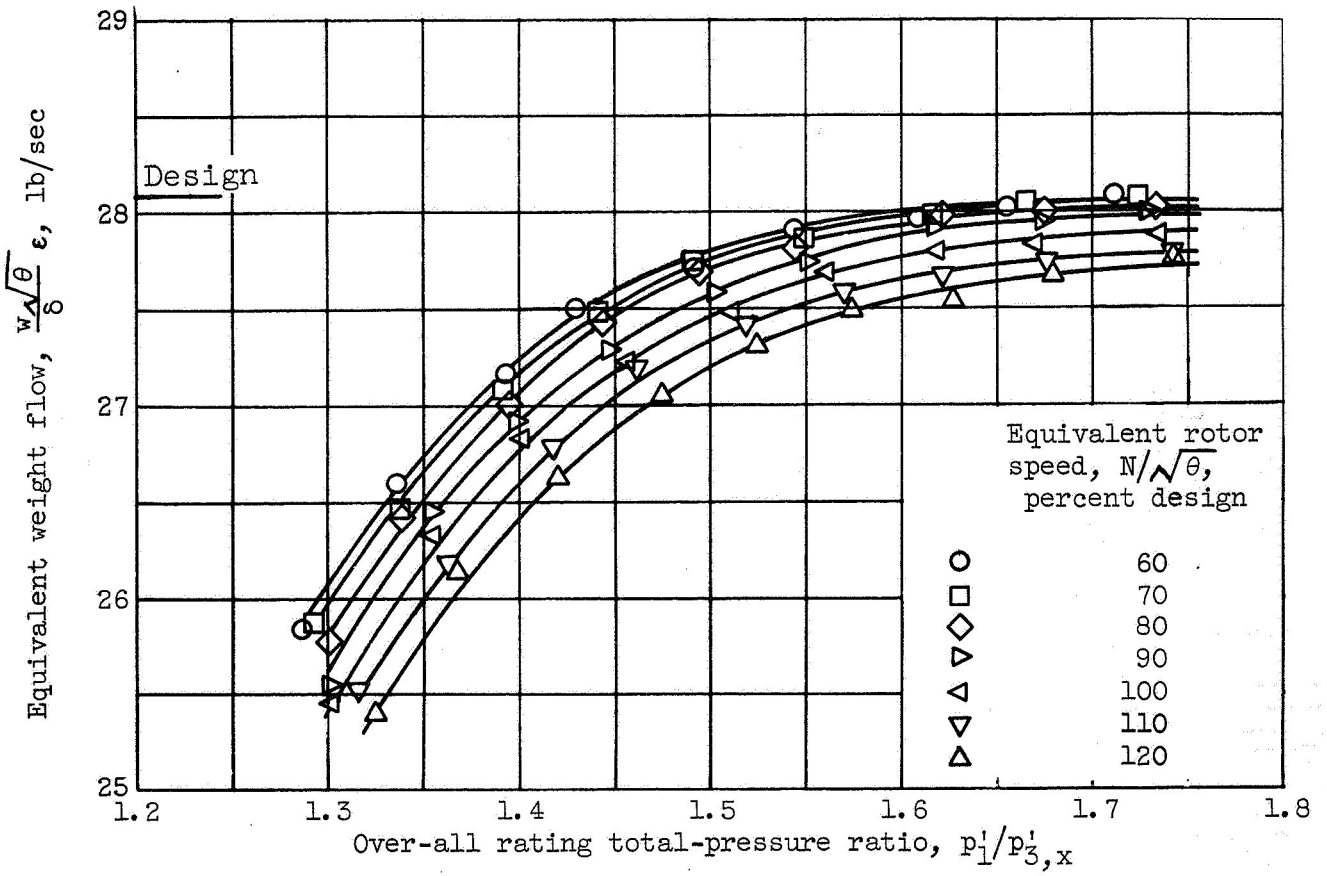

(a) Equivalent weight flow.

Figure 8. - Variation of equivalent weight flow and equivalent torque with rating total-pressure ratio for values of constant equivalent rotor speed. Rotor blade configuration II.

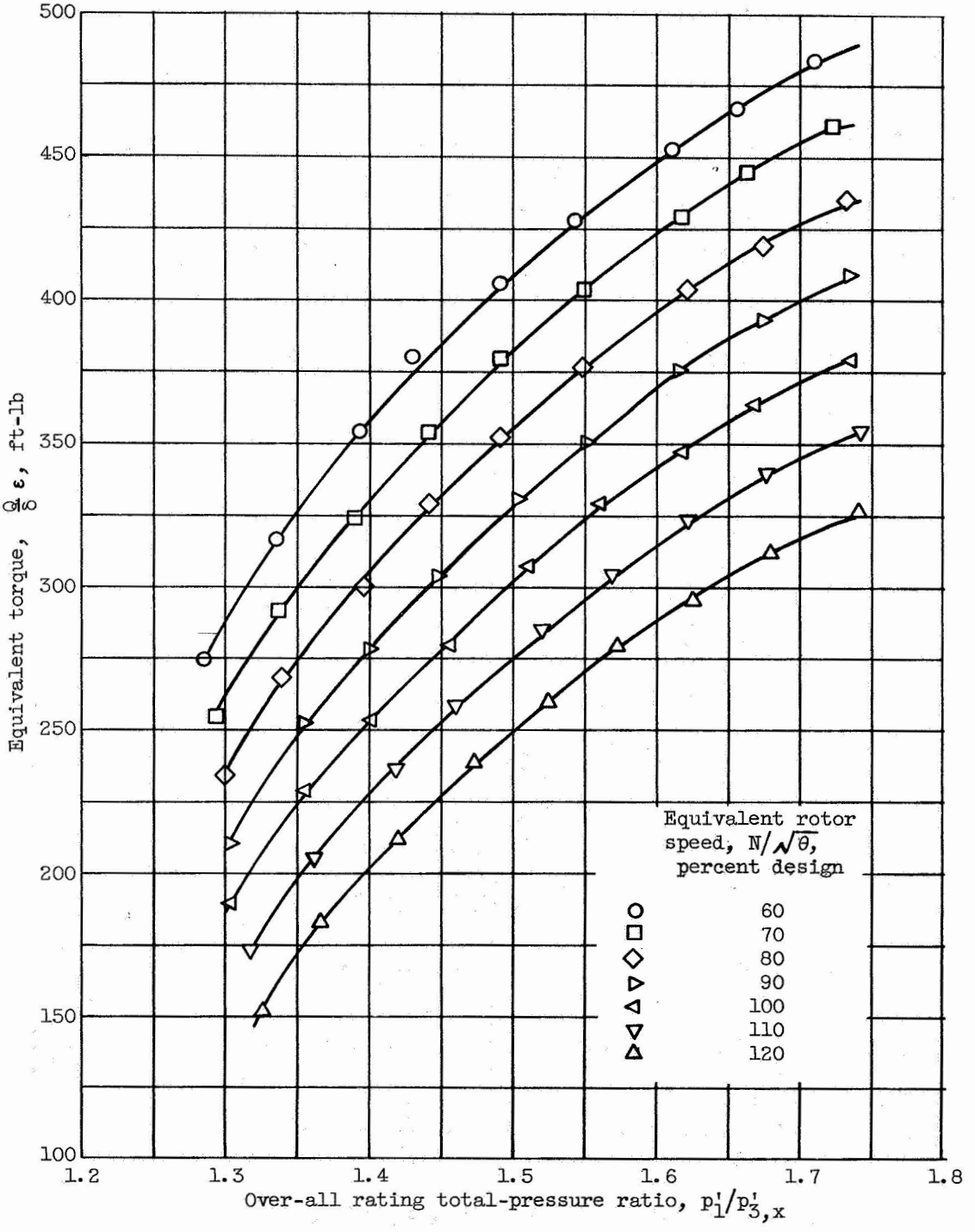

(b) Equivalent torque.

Figure 8. - Concluded. Variation of equivalent weight flow and equivalent torque with rating total-pressure ratio for values of constant equivalent rotor speed. Rotor blade configuration II.

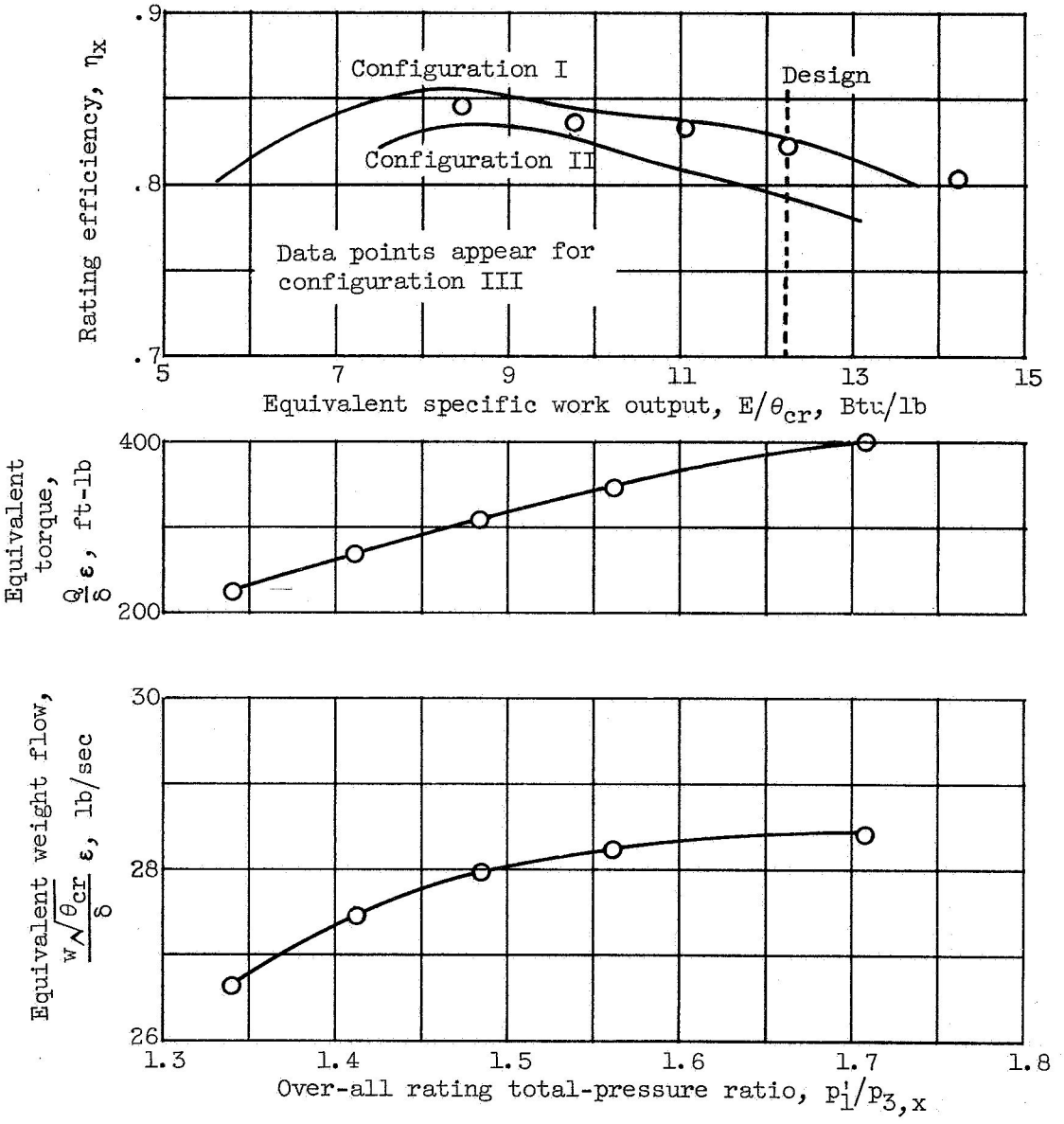

Figure 9. - Performance of turbine with rotor blade configuration III. A comparison with rotor blade configurations I and II rating efficiencies is shown. Equivalent design speed.